Supporting Information

An albumin-based nanoparticle for dual-modality imaging of the lymphatic system.

Mingze Li [a], Yundong Zhang [a], Jinli Ma [a], Jianshi Du[a, *]

[a] Jilin Provincial Key Laboratory of Lymphatic Surgical Disease, Engineering Laboratory of Lymphatic Surgery Jilin Province, China-Japan Union Hospital of Jilin University, Changchun, Jilin, 130031, P. R. China

* Corresponding author

E-mail address: dujs@jlu.edu.cn (J. Du).

1.Biological experiments

1.1 Cell experiments

Raw246.7 and HUVEC line were originally obtained from American Type Culture Collection (ATCC) and cultured in RPMI-1640 cell medium supplemented with 10% fetal bovine serum (FBS) and 1% penicillin/streptomycin under 37 ℃ within 5% CO_2. To determine the cellular uptake efficiencies, Raw246.7 and HUVEC cells pre-seeded in 24-well plates at the density of 5×10^4 cells/well were incubated with IR-780@BSA@Gd for different periods of time (1, 2, 4, 6 h). After washing cells with phosphate buffered saline (PBS) for 3 times, cells were stained with 40, 6-diamidino-2phenylindole (DAPI) and then imaged by a laser scanning confocal fluorescence microscope (Leica SP5). The in vitro cytotoxicity was measured using a standard methyl thiazolyltetrazolium (MTT, Sigmae Aldrich) assay. For cell toxicity assay,

Raw246.7 and HUVEC cells were seeded into 96-well cell culture plates at 1×10^5/well until adherent and then incubated with various concentrations of IR-780@BSA@$Gd^{3+}$for 24 h.

1.2 Animal experiments

All animal studies were conducted in accordance with the principles and procedures outlined in the National Institutes of Health (NIH) Guide for the Care and Use of Laboratory Animals and under protocols approved by the NIH Clinical Center Animal Care and Use Committee (protocol number: NIBIB 16-03). Some animal experiments were performed under the Stanford University's Administrative Panel on Laboratory Animal Care. Nude, C57, and BALB/c mice were purchased from the Jackson Laboratory (Bar Harbor, ME). Bedding, nesting material, food, and water were provided ad libitum. Ambient temperature was controlled at 20° to 22°C with 12-hour light/12-hour dark cycles.

1.3 Establishment of the mouse model of lymphedema

Methylene blue was injected subcutaneously at the footpad of the right hindlimb of mice to visualize lymph nodes and lymphatic vessels. Anesthesia was performed by intraperitoneal injection of 5% chloral hydrate. A circular incision was made at 1cm above the knee of the right hind limb, and 1cm of skin and subcutaneous tissue were excised. The neurovascular bundle muscles and tendons were carefully preserved during the operation. The popliteal lymph nodes were removed under a dissecting microscope, and the blue-stained lymphatic vessels were excised and the surrounding

skin was cauterized by electrocautery. Apply erythromycin ointment to the wound after surgery to prevent infection.

1.4 HE staining

Mice were intravenously (i.v.) injected with 400 μL IR-780@BSA@Gd^{3+} stock solution or PBS (as control), and 24 h varying tissues (i.e., liver, lung and kidney) were harvested and fixed overnight in 4% paraformaldehyde. Paraffin sections were prepared and stained with hematoxylin-eosin (H&E), and the slides were observed and photographed with optical microscope (IX71, Olympus, Tokyo, Japan).

1.5 NIR-II imaging

Mice were shaved using Nair hair removal cream (Nair Lotion with Aloe & Lanolin) and anesthetized using isoflurane before placing them in a stage with a venous catheter for injection of imaging agents. For each imaging experiment, at least three mice were used per group. All NIR-II images were collected on a two-dimensional InGaAs array (Princeton Instruments) based on a previous setup (15, 36). The excitation laser was an 808-nm laser setup at a power density of ~0.15 W/cm2. Emission was typically collected with different short/long-pass filters. A lens set was used for obtaining tunable magnifications, ranging from 1× (whole body) to 2.5× (high magnification) by changing the relative position of two NIR achromats (200 and 75 mm; Thorlabs). A variable exposure time was used for the InGaAs camera to capture images in the NIR-II window. NIR-II microscopy was built on the basis of the previous report, and the excitation laser was a 785-nm laser setup (36). PCA was performed on groups of images by considering each pixel to be an observation that

varies over the variable time. We further programmed a MATLAB command to resolve the vein and artery information. The signals in the blood vessels from the beginning of injection were completely recorded, and the profile of each blood vessel perfusion was recorded. Since intravenous injection was performed, the venous vessels were firstly detected (the venous vessels were perfused with fluorophores after injection), followed by the artery vessels. For the calculation of vessel/muscle ratio, ROIs were drawn on selected vessels and the same muscle regions. Thus, the signal intensity of vessel to that of specific muscle ratio (SBR) value was required to compare the contrasts of different fluorophores.

1.6 MRI imaging

For in vivo imaging, IR-780@BSA@Gd^{3+} were injected into the right rear footpad. The mice were imaged by a Maestro in vivo imaging system over time after injection. MR imaging was conducted by using a 3.0-T clinical MR scanner (GE healthcare, USA) equipped with a special coil for small animal imaging. After acquiring T1-weighted MR images, the signal intensity was measured within a manually drawn region of interest for each mouse.

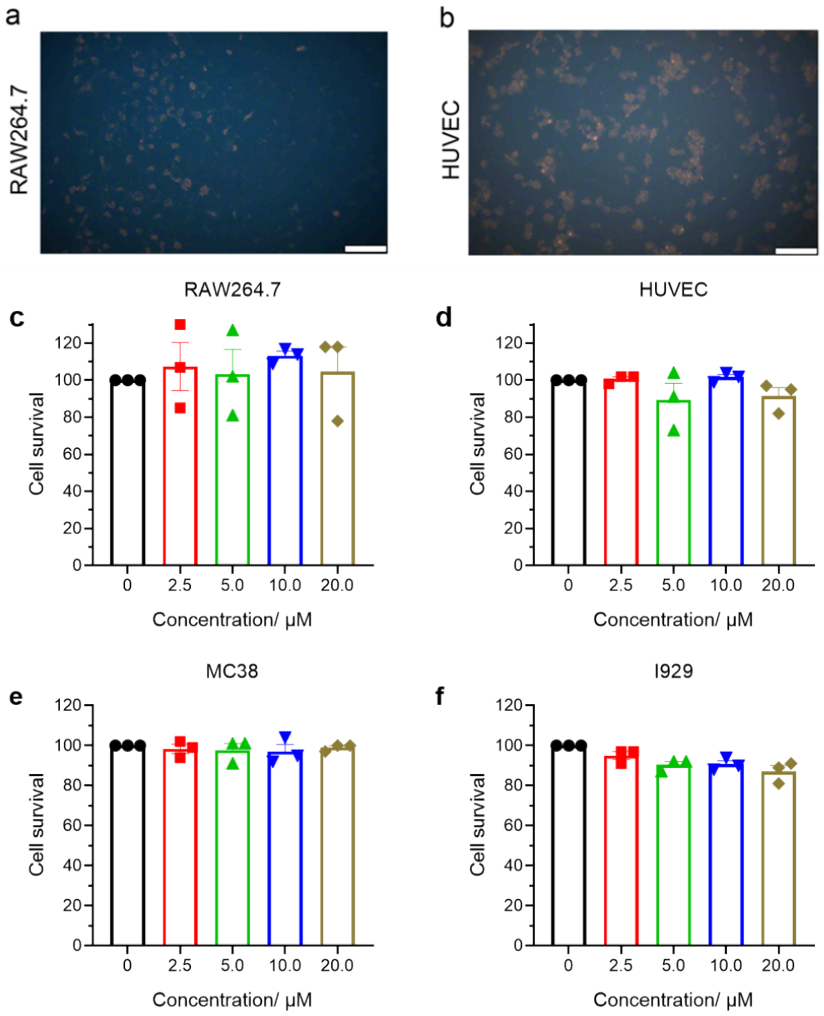

Figure S1. Biosafety assessment of IR-780@BSA@Gd^{3+} in vitro. (a). Confocal laser microscopy to observe the growth state of macrophages after co-incubation with IR-780@BSA@Gd^{3+}. **(b).** Laser confocal microscopy to observe the growth state of umbilical endothelial cells after co-incubation with IR-780@BSA@Gd^{3+}. **(c).** The cell viability of macrophages after co-incubating with different concentrations of IR-780@BSA@Gd^{3+}. **(d).** The cell viability of umbilical vascular endothelial cells after co-incubating with different concentrations of IR-780@BSA@Gd^{3+}. **(e).** The cell viability of MC38 after co-incubating with different concentrations of IR-780@BSA@Gd^{3+}. **(f).** The cell viability of I929 after co-incubating with different concentrations of IR-780@BSA@Gd^{3+}.

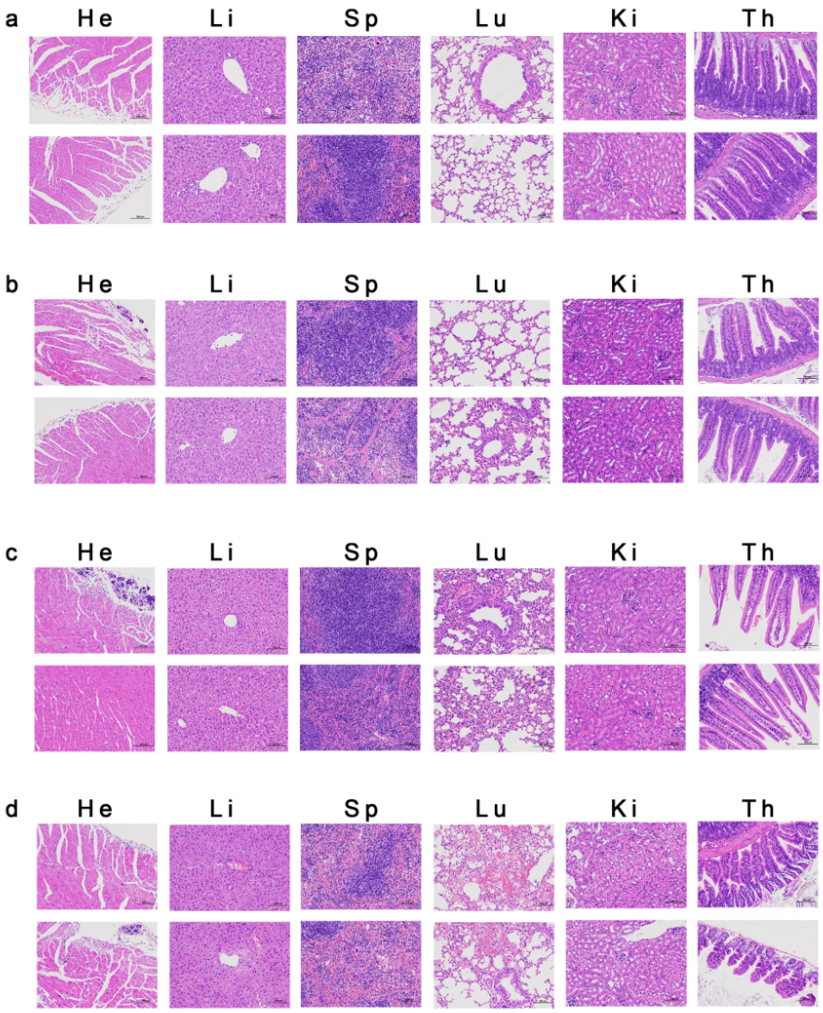

Figure S2. Biosafety assessment of IR-780@BSA@Gd^{3+} **in vivo. (a).** HE staining of each organ after 48 h injection of IR-780@BSA@Gd^{3+} into the tail vein of mice. **(b).** HE staining of each organ after 24 h injection of IR-780@BSA@Gd^{3+} into the tail vein of mice. **(c).** HE staining of each organ after 24 h injection of IR-780@ BSA into the tail vein of mice. **(d).** HE staining of each organ after 24 h injection of Free IR-780 into the tail vein of mice.

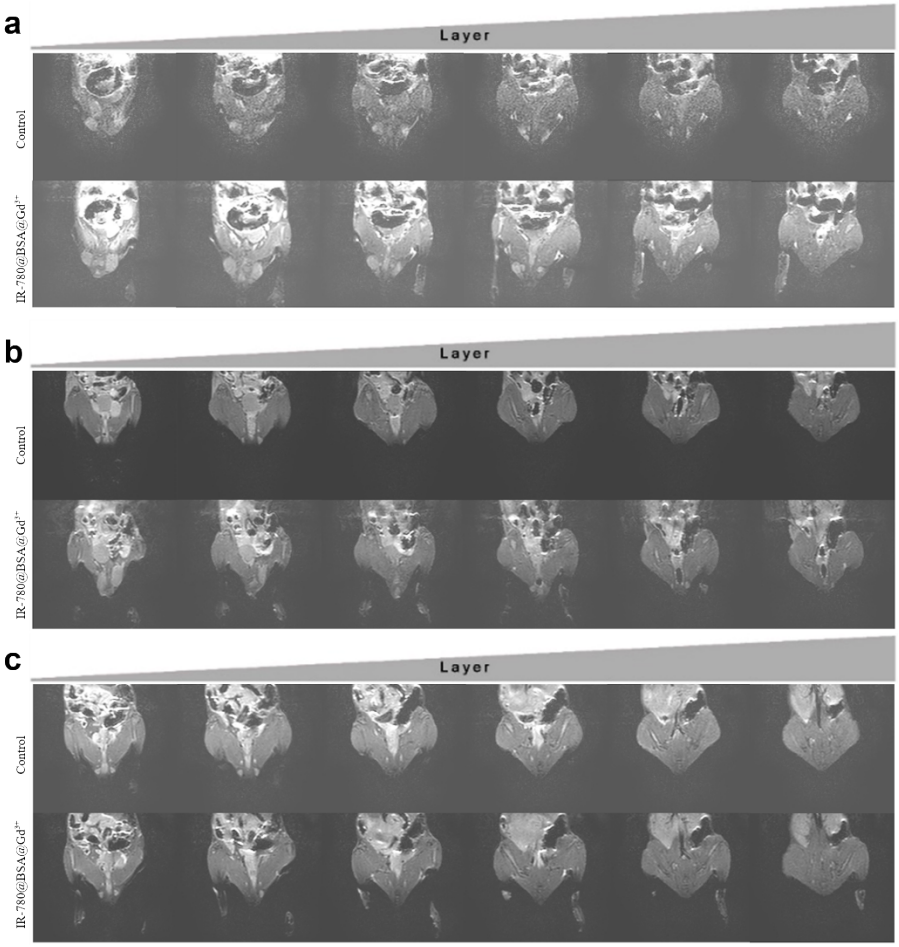

Figure S3. Lymphatic imaging of mouse bimodal complexes. (a). MRI images of mice after injection of IR-780@BSA@Gd^{3+} in the toe webs of both lower limbs of mice. **(b)(c).** Parallel Experiments in **(a).**

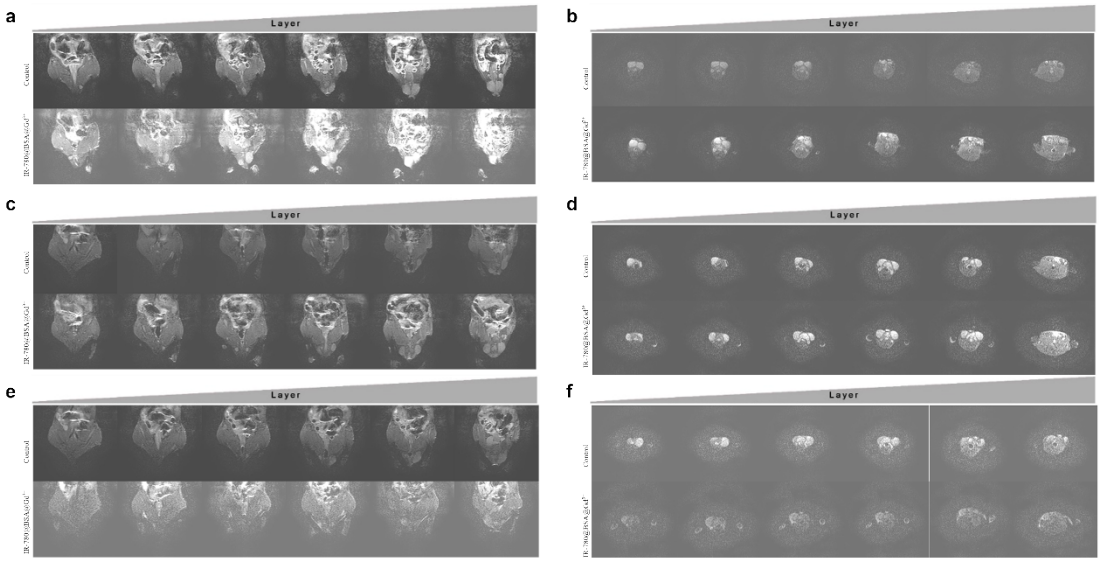

Figure S4. Lymphatic imaging of bimodal complexes in lymphedema model mice. (a). Sagittal MRI image of T1 after injection of IR-780@BSA@Gd^{3+} in the toe webs of both lower limbs of lymphedema model mice. **(b).** Axial MRI image of T1 after injection of IR-780@BSA@Gd^{3+} in the toe webs of both lower limbs of lymphedema model mice. **(c, e).** Parallel Experiments in **(a). (d, f).** Parallel Experiments in **(b).**

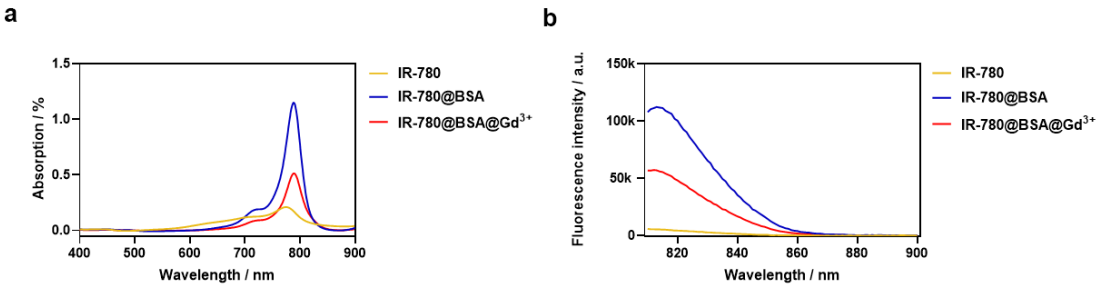

Figure S5. The absorption spectra(a)and fluorescence spectra(b)of freeIR-780，IR-780@BSA and IR-780@BSA@Gd3+ in water with thesame lR780 concentration(10um)